

Comparative Analysis of EMAT Receiving Process between Ferromagnetic and Nonferromagnetic Materials

Wei Yuan, Ze Liu, Yong Li, Jiwei Huo

School of Electronics and Information Engineering, Beijing Jiaotong University, Beijing, 100044, China

Email: zliu@bjtu.edu.cn

Abstract—The two dimensional finite element model of electromagnetic acoustic transducers (EMAT) receiving ultrasonic pulses in ferromagnetic and nonferromagnetic material were established. The model represents several significant improvements over previously published work, as follows:(a) the detail mathematical derivation and solution of key parameters in ferromagnetic and nonferromagnetic materials of test specimens have been described and compared, (b) show different propagation law which excited by EMAT in two type test specimens,(c) in order to improve the intensity of receiving signals of EMAT, orthogonal experimental analysis method is adopted to analyze the influence of different structural parameters of EMAT on receiving voltage for two kinds of tested materials. Finally, according to the characteristics of the two models, the optimal parameters are calculated. After optimization, the voltage amplitude of EMAT receiver is increased significantly. It gets 3.4 times stronger in ferromagnetic material, and 7.3 times stronger in nonferromagnetic material. (Abstract)

Keywords—electromagnetic acoustic transducer; receiving process; ferromagnetic and nonferromagnetic material (key words)

I. INTRODUCTION

Electromagnetic acoustic transducer(EMAT) is widely used due to its advantages of non-contact detection without any coupling agent or any treatment of rough surface. However, its energy transfer mechanism is complex, involving the coupling of electromagnetic field, solid mechanics field and acoustic field, and the problem of low energy transfer efficiency remains unsolved.

In order to improve the signal-to-noise ratio (SNR)of EMAT,so many attempts had been made. For instance, based on the EMAT excitation mechanism, Koorosh, KANG and DUTTON et al. established ,a numerical model and a finite element simulation model to optimize the structural parameters of EMAT by using orthogonal experimental analysis [1-3]. Starting from the hardware circuit design and noise reduction algorithm, HIRAO M and Suzhen Liu [4-6] et al. designed impedance matching network, anti-interference circuit and noise suppression algorithm to improve the received signal. In recent years, EMAT receiving process has been analyzed, but most of researches are for nonferromagnetic materials[7-8]. Nondestructive testing of rail and oil pipeline belongs to the testing of ferromagnetic material, so it is very necessary to analyze receiving process of EMAT in ferromagnetic materials.

This paper mainly describes how the transient particle displacement fields are converted into an induced voltage response in ferromagnetic material and nonferromagnetic material. And the propagation law of ultrasonic wave and the influence of EMAT parameters on the receiving performance in different materials were compared and analyzed. Finally, the optimal parameters of receiving EMAT were obtained. The study provides a theoretical reference for the understanding of the receiving mechanism and the establishment of the model for other researchers.

II. THEORY

EMAT energy exchange includes Lorentz mechanism and Magnetostriction mechanism. The former is mainly applied to nonferromagnetic materials. The later plays a dominant role in the process of excitation and reception of EMAT, when the test specimen is a ferromagnetic material, which has magnetostrictive properties.

A. Receiving mechanism of EMAT

Ultrasonic waves induce particle vibration in test specimen as they propagate through the specimen.

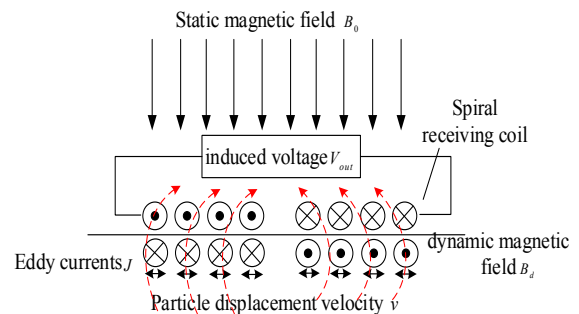


Fig. 1. EMAT receiving schematic

Eddy currents J induced in test specimen in the presence of a static magnetic field B_0 , meanwhile producing time varying magnetic fluxes B_d though the receiving coil, then a voltage V_{out} across the coil.

B. Mathematical model of EMAT

Total induced eddy current generated in the surface of the tested sample is given by:

$$J = J_L + J_M = \sigma v \times B_0 + \nabla \times B_M \quad (1)$$

Where J_L and J_M are the induced current generated by the reverse Lorentz and Magnetostrictive effect. When the tested specimen is a nonferromagnetic material, only J_L needs to be considered. And when the tested specimen is a ferromagnetic material, J_M must be taken into account. Where v and σ are the particle velocity and electrical conductivity in specimen. B_M is the magnetic induction intensity caused by the particle displacement on the material surface.

$$B_M = eS = c_{ij} d_{ki} s \quad (4)$$

The e and S are the key parameters during the establishment of the simulation model, which represent the matrix of inverse piezomagnetic and the strain tensor respectively.

Assuming that the tested specimen is isotropic, the stiffness matrix c_{ij} can be expressed as:

$$[c_{ij}] = \begin{bmatrix} c_{11} & c_{12} & c_{12} & 0 & 0 & 0 \\ c_{12} & c_{11} & c_{12} & 0 & 0 & 0 \\ c_{12} & c_{12} & c_{11} & 0 & 0 & 0 \\ 0 & 0 & 0 & c_{44} & 0 & 0 \\ 0 & 0 & 0 & 0 & c_{44} & 0 \\ 0 & 0 & 0 & 0 & 0 & c_{44} \end{bmatrix} \quad (5)$$

The inverse piezomagnetic matrix e can be expressed as :

$$e = \begin{bmatrix} 0 & 0 & 0 & 0 & 0 & c_{44} \frac{3\varepsilon_M}{H_0} \\ [c_{12} - \frac{1}{2}(c_{11} + c_{12})]\lambda_M & (c_{11} - c_{12})\lambda_M & [c_{12} - \frac{1}{2}(c_{11} + c_{12})]\lambda_M & 0 & 0 & 0 \\ 0 & 0 & 0 & c_{44} \frac{3\varepsilon_M}{H_0} & 0 & 0 \end{bmatrix} \quad (6)$$

Where c_{11} , c_{12} and c_{44} are related to the Mera constants of the tested specimen. H_0 is the corresponding magnetic field strength at B_0 in the $B-H$ curve of ferromagnetic materials. ε_M is the strain at the magnetic field strength H_0 in the $H-\varepsilon_M$ curve, and λ_M is the slope of the point.

Each region of the receiving coil and tested sample meet the governing equation:

$$-\frac{1}{\mu_t} \nabla^2 A + \sigma \frac{\partial A}{\partial t} - \frac{\sigma}{S} \frac{\partial}{\partial t} \iint_{\Omega} Ads = J \quad (7)$$

Where μ_t and A are magnetic permeability and magnetic vector potential.

The vector magnetic potential A can be obtained from (7), then the induced electric field E from the coil to the body can be expressed as:

$$E = -\frac{\partial A}{\partial t} \quad (8)$$

The electromotive force of a point can be obtained by line integral of electric field intensity in spiral coil:

$$V_{point} = \int_l -\frac{\partial A}{\partial t} dl \quad (9)$$

The output voltage of the coil can be obtained by averaging the point electromotive force contained in the coil:

$$V_{out} = \frac{\int_{\Omega} V_{point} d\Omega}{\int_{\Omega} d\Omega} \quad (10)$$

l is the length of coil, and Ω is cross-sectional area of coil.

C. Establishment of simulation model

Finite element simulation software was used to establish two two-dimensional EMAT receiving models, one for ferromagnetic materials and the other for nonferromagnetic materials. The EMAT receiving process is mainly divided into four parts: air, permanent magnet, receiving spiral coil and tested specimen. Aluminum plate and steel plate are used to replace nonferromagnetic material and ferromagnetic material as test specimen. EMAT structure diagram and optimized parameter setting are shown in the Fig.2 and Tab.1.

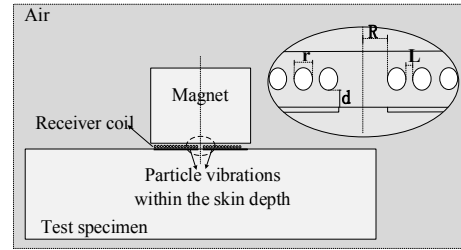


Fig. 2. Finite element simulation model

In different models, the material parameters of the tested parts are set individually. For aluminum, the Young's modulus is $70e9$ [Pa], the Poisson's ratio is 0.33 the density is 2700 [kg/m³] and the magnetic permeability is 1. For steel, the Young's modulus is 210 [GPa], the Poisson's ratio is 0.29, the density is 7850 [kg/m³] and the magnetic permeability is 400.

TABLE I. PARAMETERS TO BE OPTIMIZED

Receiving spiral coil	Parameter values(mm)
the spiral coil radius (R)	6
the wire spacing of spiral coil (L)	0.1
the wire radius (r)	0.25
lift-off (d)	0.3

III. THE COMPARISON OF THE RESULTS

A. Comparison of propagation law

After calculation, the propagation of ultrasonic wave in steel and aluminum are obtained. Under the same excitation, ultrasonic wave is generated on the surface of the tested piece

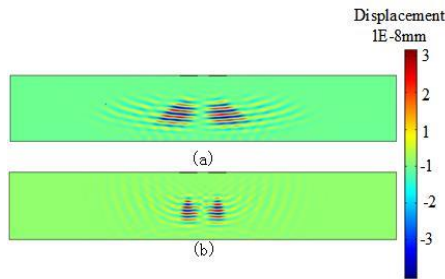


Fig. 3. The propagation law in ferromagnetic(a) and nonferromagnetic (b) material

and propagates downward. When it reaches the bottom boundary and returns immediately, which is consistent with the ultrasonic wave propagation and attenuation theory.

The propagation path is shown in Fig.3, in which we can find an angle dispersion from the propagation of ultrasound in the ferromagnetic specimen. This phenomenon does not occur in nonferromagnetic specimen.

B. Optimization comparison of spiral coil parameters

The size of the spiral coil is important parameters to determine the intensity of induction voltage of the EMAT receiver. In order to obtain the optimal parameters of the coil, this paper combines the finite element simulation software with the orthogonal experimental analysis method to extract the key parameters of the coil, and to analyze the influence degree and

change trend of the parameters on receiving performance. The research mainly focuses on peak-to-peak value U_{pp} (U_{fpp} stands for the U_{pp} in ferromagnetic specimen and U_{lpp} stands for the U_{pp} in nonferromagnetic specimen) of the induced voltage in the receiving coil, and four factors are considered on U_{pp} : the inner radius (R) of the spiral coil, the lift-off (d), the coil radius (r), and the line spacing (L).

According to the common specifications and manufacturing process of received EMAT the value range of each factor was determined. Within each range: R: 2-5mm, d: 0.1-0.7mm, R: 0.2-0.8mm, L: 0.1-0.7mm, each factor is taken as 4 values, forming the orthogonal analysis table as shown in Tab.2. According to the orthogonal test results, the average value K_i of U_{pp} under the same parameters is obtained, and the extreme difference of different factors is obtained, as shown in Tab.3.

TABLE II. ORTHOGONAL TEST OF 4 ELEMENTS 4 LEVELS FOR RECEIVING

	L (mm)	R (mm)	r (mm)	d (mm)	U_{fpp} ($10^{-4}V$)	U_{lpp} ($10^{-5}V$)
1	0.1	2	0.2	0.1	6.34	2.96
2	0.1	3	0.4	0.3	3.43	2.12
3	0.1	4	0.6	0.5	1.73	0.997
4	0.1	5	0.8	0.7	0.978	0.554
5	0.3	2	0.4	0.3	2.51	1.65
6	0.3	3	0.2	0.1	5.36	3.44
7	0.3	4	0.8	0.7	0.834	0.472
8	0.3	5	0.6	0.5	1.29	0.710
9	0.5	3	0.6	0.3	1.14	0.611
10	0.5	2	0.8	0.1	0.799	0.304
11	0.5	5	0.4	0.7	1.63	0.951
12	0.5	4	0.2	0.5	3.25	2.00
13	0.7	4	0.8	0.1	0.604	0.256
14	0.7	5	0.6	0.7	0.806	0.447
15	0.7	2	0.4	0.3	1.50	0.875
16	0.7	3	0.2	0.5	2.50	1.53

TABLE III. ANALYSIS OF ORTHOGONAL TEST FOR RECEIVING EMAT

	L		R		r		d	
	U_{fpp}	U_{lpp}	U_{fpp}	U_{lpp}	U_{fpp}	U_{lpp}	U_{fpp}	U_{lpp}
k1	3.12	1.653	2.787	1.448	4.363	2.482	3.278	1.740
K2	2.499	1.568	3.108	1.93	2.268	1.399	2.145	1.314
K3	1.705	0.967	1.605	0.931	1.242	0.691	2.193	1.309
K4	1.353	0.77	1.176	0.666	0.804	0.396	1.062	0.606
range	1.767	0.876	1.932	0.786	3.559	2.086	2.216	1.134

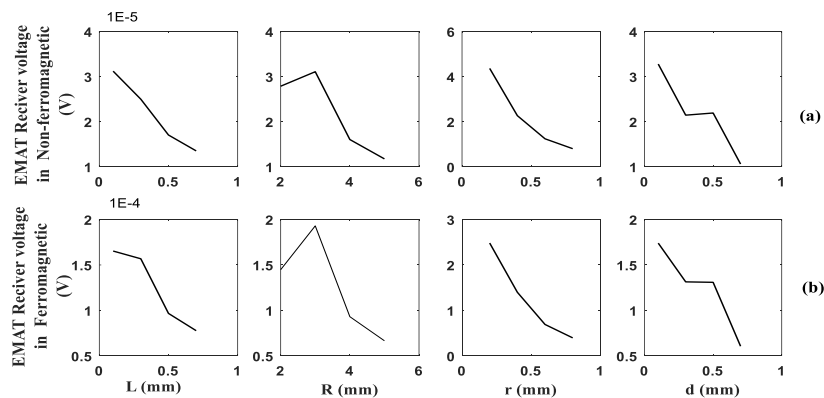


Fig. 4. Trend curves of EMAT receiver voltage in different structural parameters. The first row represents non-ferromagnetic material(a), and the second row represents ferromagnetic material(b)

The orthogonal experimental analysis table shows that the influence degree of the wire radius(r), lift-off(d), the wire spacing of the spiral coil(L) and the spiral coil radius(R) decreases in turns ($r(3.559)>d(2.216)>R(1.932)>L(1.767)$) on the receiving voltage in ferromagnetic material. The influence in nonferromagnetic material has a similar scale to that in ferromagnetic materials ($r(2.086)>d(1.134)>L(0.876)>R(0.786)$), with the most visible difference being for L and R , which is 0.09. The trend chart of each factor changing with its parameter can be obtained from Tab.3, as shown in Fig. 4. It can be seen that the receiving induced voltage decreases with the increase of L , R , r and d . When $R=3\text{mm}$, the receiving induced voltage has a peak value. Meanwhile, the internal radius of excited EMAT is also 3mm. Therefore, it is concluded that the smaller the structure of received EMAT is, the more concentrated the energy is, and the higher the voltage signal strength is. Finally, the optimal parameter of the spiral is $r=0.1\text{mm}$, $R=3\text{mm}$, $L=0.2\text{mm}$, $D=0.1\text{mm}$.

C. Comparison of receive voltage signal

When it comes to the transduction efficiency of EMAT, researchers often use the particle displacement amplitude to judge the strength of the received signal. However, not the particle displacement amplitude but particle vibrations velocity within the skin depth of the specimen can produce an effective contribution to the induced voltage. So the induce voltage is uniqueness theoretical basis for the design to optimize EMAT and improve SNR.

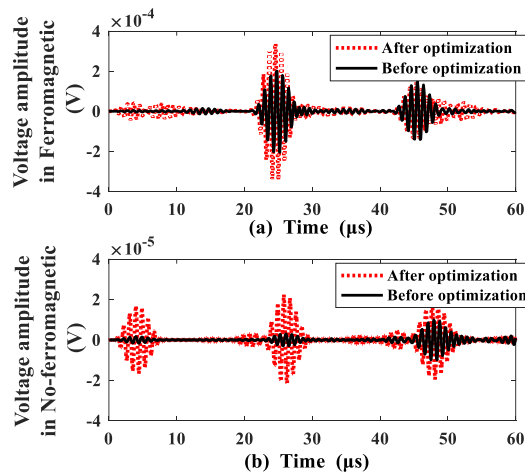


Fig. 5. Comparison diagram of induced voltage amplitude before and after optimization

Fig.5 is the comparison diagram of receiving induced voltage amplitude before and after optimization in (a) ferromagnetic material and (b) nonferromagnetic material. Due to the existence of inverse magnetostrictive effect, the induced voltage signal in ferromagnetic material is stronger than that in nonferromagnetic material. The inverse magnetostrictive current plays an important role. However, the induced voltage of the optimized coil increases more strongly in nonferromagnetic material than that in ferromagnetic material.

IV. CONCLUSION

The mathematical derivation and solution of key parameters in ferromagnetic tested specimens have been described and complete simulation modeling systems have been developed for EMAT receiver operating in nonferromagnetic and ferromagnetic specimen. Although some models and papers have been attempted previously, this is the first time to include the comparison of receiving process for two materials. Such comparison is essential to allow optimal design of EMAT in different scenarios. To our surprise, waves travel in different paths in different materials under the same EMAT excitation. Certain dispersion angles occur in ferromagnetic materials, but not in other materials. Finally, the influence degree of spiral coil parameters on EMAT receiving coil induced voltage is compared. After optimization, the voltage amplitude of EMAT receiver is increased significantly. It gets 3.4 times stronger in ferromagnetic material, and 7.3 times stronger in nonferromagnetic material. It is concluded that the smaller the structure parameters of the EMAT receiver, are the stronger the received signal will be.

ACKNOWLEDGMENT

This work is supported by Natural Science Foundation of Beijing(4198045) and Science Foundation of China (61771041).

REFERENCES

- [1] Koorosh Mirkhani, Chris Chaggares, et. Optimal design of EMAT transmitter[J]. NDT&E International,37(2004). 181-193.
- [2] KANG Lei, DIXON S, WANG Kaican, et al. Enhancement of signal amplitude of surface wave EMATs based on 3-Dsimulation analysis and orthogonal test method[J]. NDT & E International, 2013, 59(7): 11 – 17.
- [3] DUTTON B, BOONSANG S, DEWHURST R J. A new magnetic configuration for a small in-plane electromagnetic acoustic transducer applied to laser-ultrasound measurements:modelling and validation[J]. Sensors & Actuators A: Physical, 2006, 125(2): 249 – 259.
- [4] HIRAO M, OGI H. EMATS for science and industry non-contacting ultrasonic measurements[M]. Boston: KluwerAcademic Publisher, 2003: 73 – 80.
- [5] Liu Shuzhen, Li Libin, Cai Zhichao, et al. The design for electromagnetic interference eliminating circuits in electromagnetic ultrasonic testing systems[J]. Transactions of China Electrotechnical Society, 2016, 31(1): 80 – 84.
- [6] WANG Yakun. Anti-interference design of EMAT reception system and research on noise reduction algorithm[D]. Harbin Institute of Technology. School of Electrical Engineering and Automation, 2014: 51 – 64.
- [7] SHI Wenze, WU Yunxin,et. Circuit-field coupled analysis of receiving efficiency of spiral coil electromagnetic acoustic transducer in non-ferromagnetic metal material [J]. Journal of Central South University (Science and Technology) , 48(12)2017 : 3200-3208.
- [8] Sun Wenxiu, Liu Guoqiang, et. Numerical Simulation and Experimental Study of Electromagnetic Acoustic Transducer Receiving Process in Nonferromagnetic Material[J]. Transactions of China Electrotechnical Society,2018,33(19): 4443-4449.